Journal of Advanced Research in Applied Mechanics

Journal homepage:
https://semarakilmu.com.my/journals/index.php/appl_mech/index
ISSN: 2289-7895

Multiple Inclined Edge Cracks in Two Bonded Half-Planes Subjected to Normal Stress

Nur Hazirah Husin[1], Nik Mohd Asri Nik Long[1,2,*], Norazak Senu[1,2], Khairum Hamzah[3,4]

1 Institute for Mathematical Research, Universiti Putra Malaysia, 43400 UPM Serdang, Selangor, Malaysia
2 Department of Mathematics and Statistics, Faculty of Science, Universiti Putra Malaysia, 43400 UPM Serdang, Selangor, Malaysia
3 Faculty of Mechanical and Manufacturing Engineering Technology, Universiti Teknikal Malaysia Melaka, Hang Tuah Jaya, Durian Tunggal, 76100, Melaka, Malaysia
4 Forecasting and Engineering Technology Analysis (FETA) Research Group, Universiti Teknikal Malaysia Melaka, Hang Tuah Jaya, Durian Tunggal, 76100, Melaka, Malaysia

ARTICLE INFO

Article history:
Received 21 October 2024
Received in revised form 22 December 2024
Accepted 29 December 2024
Available online 30 January 2025

Keywords:
Edge crack; normal stress; modified complex potentials; singular integral equation; two bonded half-planes; stress intensity factor

ABSTRACT

This paper considers multiple inclined edge cracks under normal stress originating at the interface of two bonded half-planes. The crack problem is formulated into the singular integral equation (SIE) using a modified complex potential (MCP) with the conditions of continuity for traction and displacement. A semi-open quadrature approach is applied for the numerical solution of the SIE. The behavior of stress intensity factors (SIFs) for both Modes I and II at all crack tips is computed and demonstrated graphically. The crack configuration, the elastic constant ratios of the planes, the inclination angle, and the distance between cracks have significantly influenced Modes I and II SIFs. By analyzing the behavior of SIF near the crack tip, engineers may predict the lifespan of the building structures.

1.Introduction

Cracks or flaws may affect material durability, thereby jeopardizing the lifespan of building structures. Engineers can predict the propagation of cracks under different loading conditions by understanding the stress intensity factor (SIF), which is vital for analyzing the strength and durability of materials. It helps to determine whether a detected crack will remain stable or whether material poses a significant risk of catastrophic failure, such as structural damage and human death. Therefore, evaluating SIF is necessary for examining materials containing cracks. A number of researchers have conducted several studies on the behavior of SIF on many types of single and multiple cracks under different forms of stress.

An anisotropic material with an oblique edge crack subjected to shear stress was formulated by Beom and Cui [1] using the linear transformation method. Mode III of SIF for the oblique edge crack

* *Corresponding author.*
E-mail address: nmasri@upm.edu.my

https://doi.org/10.37934/aram.132.1.7082

was calculated numerically. Hello *et al.,* [2] presented the explicit formulas for every coefficient in the Laurent and power series of a single finite crack on an infinite plane due to the remote stress of Modes I and II. The analysis of a single inclined crack on a finite plane under biaxial tensile loads was discussed by Li *et al.,* [3], and SIF was calculated using the distributed dislocation approach together with the Gauss-Chebyshev quadrature formula. Yu *et al.,* [4] proposed a circular arc crack in the thermoelectric plane under electrical and thermal loads. Meanwhile, Hasebe [5] investigated a half-plane weakens by a vertical crack by applying a polygonal mapping function that was formulated through Schwarz-Christoffel's transformation. Subbaiah and Bollineni [6] used numerical modeling and a 2D axisymmetric finite element framework to analyze the SIF for an inclined edge crack that occurs on a cylinder pressure vessel while also performing the fracture analysis. In addition, the mechanical analysis of a kinked crack was studied by Liu and Wei [7] using conformal mapping and the complex variable function approach. Singh and Das [8] examined a partially insulated crack in a composite structure consisting of a pair of functionally graded strips of a random orientation that undergo thermomechanical loading. An inclined crack in thermoelectric bonded planes under remote stress was presented by Nordin *et al.,* [9]. Recently, Husin *et al.,* [10] considered a single-edge crack in two bonded half-planes undergoing shear stress.

Furthermore, Jin and Keer [11] investigated multiple edge cracks on a semi-infinite plane subjected to constant stress using the distributed dislocation method. Hypersingular integral equations were applied to formulate multiple curved [12], inclined, and circular arc crack [13] problems. Multiple edge cracks and arbitrarily hole problems that are transversely isotropic and have piezoelectric properties caused by in-plane electrical and out-plane shear loads were explored by Wang *et al.,* [14] using the numerical conformal mapping approach and the complex variable method. Choi [15] carried out parametric studies to address the problem of multiple parallel, edge-interfacial cracks caused by antiplane deformation, while Mode III SIF was taken into account. Moreover, an analysis is conducted by Stepanova and Roslyakov [16] to derive and examine the multiparametric representation of the stress distribution for multiple parallel cracks of finite lengths in an infinite plate due to mixed loading conditions. An automated numerical model of a finite plane with multiple kinked and straight cracks under uniform tensile stress was developed by Zhang *et al.,* [17] using the distributed dislocation technique (DDT). Based on DDT, Moradi and Monfared [18] studied the multiple curved cracks in an orthotropic functionally graded material (FGM) layer that was bonded to a different orthotropic layer. They computed the SIFs for Modes I and II as well as the energy of strain transfer rates.

However, there is limited research on multiple inclined edge cracks in two bonded half-planes. This paper presents the multiple edge cracks that originate at the interface of two bonded half-planes, (i) towards the upper half of the planes and (ii) towards the upper and lower planes subjected to normal stress. The behavior of SIFs for Modes I and II on the inclination angle, the distance between cracks, and the elastic constant ratios of the planes is graphically described.

2. Mathematical Formulation

The complex variable function method is derived using the complex potential functions $\Phi(\zeta), \Psi(\zeta)$ with $\phi'(\zeta), \psi'(\zeta)$ corresponding to resultant force functions (X, Y), displacements (u, v), and stresses $(\sigma_x, \sigma_y, \sigma_{xy})$ as follows [19]:

$$\sigma_x + \sigma_y = 4Re\phi'(\zeta) \tag{1}$$

$$\sigma_y - \sigma_x + 2i\sigma_{xy} = 2[\bar{\zeta}\Phi'(\zeta) + \Psi(\zeta)] \tag{2}$$

$$-Y + iX = \phi(\zeta) + \xi\overline{\phi'(\zeta)} + \overline{\psi(\zeta)} \tag{3}$$

$$2G(u + iv) = \kappa\phi(\zeta) - \zeta\overline{\phi'(\zeta)} - \overline{\psi(\zeta)} \tag{4}$$

where G abbreviates the elastic shear modulus, v denotes the Poison's ratio, plane stress and strain problems represent by $\kappa = (3 - v)/(1 + v)$ and $\kappa = 3 - 4v$, accordingly. A bar placed over a function implies the complex conjugate of that function. Differentiating Eq. (3) with respect to ζ obtainable the following expression.

$$J\left(\zeta, \bar{\zeta}, \frac{d\bar{\zeta}}{d\zeta}\right) = \frac{d}{d\zeta}(-Y + iX) = \Phi'(\zeta) + \overline{\phi'(\zeta)} + \frac{d\bar{\zeta}}{d\zeta}\left(\zeta\overline{\phi''(\zeta)} + \overline{\psi'(\zeta)}\right) = N + iT \tag{5}$$

In Eq. (5), the defined traction functions are normal (N) and tangential (T).

For a crack problem in a half-plane, the modified complex potential (MCP) is utilized. MCP consists of two different parts: the principal and complementary, which are represented as follows.

$$\phi(\zeta) = \phi_p(\zeta) + \phi_c(\zeta) \tag{6}$$

$$\psi(\zeta) = \psi_p(\zeta) + \psi_c(\zeta) \tag{7}$$

In the original infinite plane problem, the dislocation distribution function $g'(t)$ along the crack deduces the principal part. The complementary part removes the traction that the principal part exerts on the boundary between the two planes. The complex potentials for both parts are expressed below.

$$\phi'_p(\zeta) = \frac{1}{2\pi}\int_L \frac{g'(t)dt}{t-\zeta} \tag{8}$$

$$\psi'_p(\zeta) = \frac{1}{2\pi}\int_L \frac{\overline{g'(t)}\,\overline{dt}}{t-\zeta} - \frac{1}{2\pi}\int_L \frac{\bar{t}g'(t)\overline{dt}}{(t-\zeta)^2} \tag{9}$$

$$\phi'_c(\zeta) = -\overline{\phi'_p}(\zeta) - \overline{\psi'_p}(\zeta) - \xi\overline{\phi''_p}(\zeta) \tag{10}$$

$$\psi'_c(\zeta) = \overline{\psi_p}(\zeta) + 3\zeta\overline{\phi''_p}(\zeta) + \xi\overline{\psi''_p}(\zeta) + \zeta^2\overline{\phi'''_p}(\zeta) \tag{11}$$

The unknown distribution function, $g'(t)$, is explained by:

$$g'(t) = -\frac{2Gi}{\kappa+1}\frac{d[(u(t)+iv(t))^+ - (u(t)+iv(t))^-]}{dt}, \quad t \in L, \tag{12}$$

L is the configuration of crack. $(+)$ and $(-)$ subscripts signify the upper and lower crack's faces accordingly.

For the edge crack problem, the substitutions applied in Eqs. (8) and (9) are as follows [20].

$$\phi'_p(\zeta) = \frac{\exp(i\alpha)}{2\pi}\int_0^a \frac{g'(s)ds}{T_s-\zeta} \tag{13}$$

$$\psi'_p(\zeta) = \frac{\exp(-i\alpha)}{2\pi}\int_0^a \frac{\overline{g'(s)}ds}{T_s-\zeta} - \frac{\exp(i\alpha)}{2\pi}\int_0^a \frac{\overline{T_s}g'(s)ds}{(T_s-\zeta)^2} \tag{14}$$

t is replaced with T_s, where $T_s = e + s\exp(i\alpha)$, and dt is replaced with $\exp(ia)ds$ in the above Eqs. (13) and (14). A single edge crack emerges at the interface of two bonded planes in the upper half of the planes. MCP is obtainable as follows [21].

$$\phi_1(\zeta) = \phi_{1p}(\zeta) + \phi_{1c}(\zeta) \tag{15}$$

$$\psi_1(\zeta) = \psi_{1p}(\zeta) + \psi_{1c}(\zeta) \tag{16}$$

The complex potentials in the lower part are denoted by ϕ_2 and ψ_2. The following is a representation of the continuity conditions for the resultant force in Eq. (3) and the displacements in Eq. (4), accordingly.

$$\left[\phi_1(\zeta) + \zeta\overline{\phi'_1(\zeta)} + \overline{\psi_1(\zeta)}\right]^+ = \left[\phi_2(\zeta) + \zeta\overline{\phi'_2(\zeta)} + \overline{\psi_2(\zeta)}\right]^-, \;\; T_s \,\epsilon\, L \tag{17}$$

$$G_2\left[\kappa_1\phi_1(\zeta) - \zeta\overline{\phi'_1(\zeta)} - \overline{\psi_1(\zeta)}\right]^+ = G_1\left[\kappa_2\phi_2(\zeta) - \zeta\overline{\phi'_2(\zeta)} - \overline{\psi_2(\zeta)}\right]^-, \; T_s \,\epsilon\, L. \tag{18}$$

By substituting Eqs. (15) and (16) into Eqs. (17) and (18), the following expressions yield:

$$\phi_{1c}(\zeta) = \delta_1\left[\zeta\overline{\phi'_{1p}}(\zeta) + \overline{\psi'_{1p}}(\zeta)\right] \tag{19}$$

$$\psi_{1c}(\zeta) = \delta_2\zeta\overline{\phi_{1p}}(\zeta) - \delta_1\left[\zeta\overline{\phi'_{1p}}(\zeta) + \zeta^2\overline{\phi''_{1p}}(\zeta) + \zeta\overline{\psi'_{1p}}(\zeta)\right] \tag{20}$$

$$\phi_2(\zeta) = (1+\delta_2)\phi_{1p}(\zeta) \tag{21}$$

$$\psi_2(\zeta) = (1+\delta_1)\psi_{1p}(\zeta) + (\delta_1 - \delta_2)\left(\zeta\phi'_{1p}(\zeta)\right) \tag{22}$$

where δ_1 and δ_2 are the bi-elastic constants as follows.

$$\delta_1 = \frac{G_2 - G_1}{G_1 + \kappa_1 G_2}\,, \delta_2 = \frac{\kappa_1 G_2 - \kappa_2 G_1}{G_2 + \kappa_2 G_1} \tag{23}$$

The formulation of the singular integral equation (SIE) for a single edge crack in two bonded half-planes includes a pair of components, particularly $[N(s_0) + iT(s_0)]_{1p}$ and $[N(s_0) + iT(s_0)]_{1c}$. By substituting Eqs. (13) and (14) into Eq. (5), taking the limit as s approaches s_0, the traction of the principal component can be obtained as:

$$[N(s_0) + iT(s_0)]_{1p} = \frac{1}{\pi}\int_0^a \frac{g'(s)ds}{s - s_0} + \frac{1}{\pi}\int_0^a P_1(s, s_0)g'(s)ds + \frac{1}{\pi}\int_0^a P_2(s, s_0)\overline{g'(s)}ds \tag{24}$$

where:

$$P_1(s, s_0) = \frac{\exp(i\alpha)}{2}\left(\frac{1}{T_s - T_{s_0}} + \exp(-2i\alpha)\frac{1}{\bar{T}_s - \bar{T}_{s_0}}\right)$$

$$P_2(s, s_0) = \frac{\exp(-i\alpha)}{2}\left(\frac{1}{\bar{T}_s - \bar{T}_{s_0}} - \exp(-2i\alpha)\frac{T_s - T_{s_0}}{(\bar{T}_s - \bar{T}_{s_0})^2}\right).$$

Implementing Eqs. (19) and (20) into Eq. (5), associated with Eqs. (13) and (14), and taking the limit as s approaches s_0, the complementary component is obtained as follows:

$$[N(s_0)+iT(s_0)]_{1c} = \frac{1}{\pi}\int_0^a \frac{g'(s)ds}{s-s_0} + \frac{1}{\pi}\int_0^a \big(Q_1(s,s_0)+Q_2(s,s_0)\big)g'(s)ds + \\ +\frac{1}{\pi}\int_0^a \big(Q_3(s,s_0)+Q_4(s,s_0)\big)\overline{g'(s)}ds \quad (25)$$

where:

$$Q_1(s,s_0) = \frac{\exp(i\alpha)}{2}\left\{\delta_1\left[\frac{1}{\overline{T_s}-T_{s_0}} + \frac{1}{T_s-\overline{T}_{s_0}} + \frac{\overline{T}_{s_0}-\overline{T}_s}{(T_s-\overline{T}_{s_0})^2}\right]\right\}$$

$$Q_2(s,s_0) = \frac{\exp(i\alpha)}{2}\left\{\exp(-2i\alpha)\left[\delta_1\left(\frac{\overline{T}_s-3\overline{T}_{s_0}}{(T_s-\overline{T}_{s_0})^2} - \frac{1}{T_s-\overline{T}_{s_0}} + \frac{2\overline{T}_{s_0}(\overline{T}_s-\overline{T}_{s_0})}{(T_s-\overline{T}_{s_0})^3} + \frac{2T_{s_0}(T_s-\overline{T}_s)}{(T_s-\overline{T}_{s_0})^3}\right) + \delta_2\left(\frac{1}{T_s-\overline{T}_{s_0}}\right)\right]\right\}$$

$$Q_3(s,s_0) = \frac{\exp(-i\alpha)}{2}\left\{\delta_1\left[\frac{1}{T_s-\overline{T}_{s_0}} + \frac{1}{\overline{T}_s-T_{s_0}} + \frac{T_{s_0}-T_s}{(\overline{T}_s-T_{s_0})^2} + \right]\right\}$$

$$Q_4(s,s_0) = \frac{\exp(-i\alpha)}{2}\left\{\exp(-2i\alpha)\left[\delta_1\left(\frac{T_{s_0}-\overline{T}_{s_0}}{(T_s-\overline{T}_{s_0})^2} - \frac{1}{T_s-\overline{T}_{s_0}}\right)\right]\right\}.$$

Combining both components yield

$$[N(s_0)+iT(s_0)] = \frac{1}{\pi}\int_0^a \frac{g'(s)ds}{s-s_0} + \frac{1}{\pi}\int_0^a \mu_1(s,s_0)g'(s)ds + \frac{1}{\pi}\int_0^a \mu_2(s,s_0)\overline{g'(s)}ds \quad (26)$$

where:

$$\mu_1(s,s_0) = P_1(s,s_0) + Q_1(s,s_0) + Q_2(s,s_0)$$

$$\mu_2(s,s_0) = P_2(s,s_0) + Q_3(s,s_0) + Q_4(s,s_0).$$

For the multiple edge cracks, the formulation of SIE is established from two groups of $N+iT$ and comprised of four components, which are $[N(s_{10})+iT(s_{10})]_{11}$, $[N(s_{10})+iT(s_{10})]_{12}$, $[N(s_{20})+iT(s_{20})]_{22}$ and $[N(s_{20})+iT(s_{20})]_{21}$. $[N(s_{j0})+iT(s_{j0})]_{jp}$ and $[N(s_{j0})+iT(s_{j0})]_{jc}$ represent the traction of principal and complementary parts, respectively when the observation point is applied at s_{j0} for crack-L_j for $j=1,2$. The SIEs for crack-L_1 in the upper part of two bonded half-planes yield

$$[N(s_{10})+iT(s_{10})]_1 = [N(s_{10})+iT(s_{10})]_{11} + [N(s_{10})+iT(s_{10})]_{12} \\ = \frac{1}{\pi}\int_{L_1}\frac{g_1'(s_1)ds_1}{s_1-s_{10}} + \frac{1}{\pi}\int_{L_1}\mu_1(s_1,s_{10})g_1'(s_1)ds_1 + \frac{1}{\pi}\int_{L_1}\mu_2(s_1,s_{10})\overline{g_1'(s_1)}\,ds_1 \\ +\frac{1}{\pi}\int_{L_2}\frac{g_2'(s_2)ds_2}{s_2-s_{10}} + \frac{1}{\pi}\int_{L_2}\mu_1(s_2,s_{10})g_2'(s_2)ds_2 + \\ \frac{1}{\pi}\int_{L_2}\mu_2(s_2,s_{10})\overline{g_2'(s_2)}\,ds_2. \quad (27)$$

and the SIEs for crack-L_2 in the upper part of two bonded half-planes yield

$$\begin{aligned}[N(s_{20})+iT(s_{20})]_2 &= [N(s_{20})+iT(s_{20})]_{22}+[N(s_{20})+iT(s_{20})]_{21}\\ &= \frac{1}{\pi}\int_{L_2}\frac{g_2{}'(s_2)ds_2}{s_2-s_{20}}+\frac{1}{\pi}\int_{L_2}\mu_1(s_2,s_{20})g_2{}'(s_2)ds_2\\ &+\frac{1}{\pi}\int_{L_2}\mu_2(s_2,s_{20})\overline{g_2{}'(s_2)}\,ds_2+\frac{1}{\pi}\int_{L_1}\frac{g_1{}'(s_1)ds_1}{s_1-s_{20}}\\ &\frac{1}{\pi}\int_{L_1}\mu_1(s_1,s_{20})g_1{}'(s_1)ds_1+\\ &\frac{1}{\pi}\int_{L_1}\mu_2(s_1,s_{20})\overline{g_1{}'(s_1)}\,ds_1. \end{aligned} \tag{28}$$

For the multiple edge cracks that originate at the interface of two bonded planes towards the upper and lower parts of the planes, four traction components, $\left[N(s_{j0})+iT(s_{j0})\right]_{jk}$ for $j=1,2$, $k=1,2$ that comprise two groups of $N+iT$ effects are defined. Those first two components $[N(s_{10})+iT(s_{10})]_{11}$ and $[N(s_{20})+iT(s_{20})]_{21}$ will be attained as the observation point is located at $s_{10}\epsilon L_1$ and $s_{20}\epsilon L_2$, accordingly that influenced by $g_1{}'(s_1)$ at $s_1\epsilon L_1$. The second two components $[N(s_{10})+iT(s_{10})]_{12}$ and $[N(s_{20})+iT(s_{20})]_{22}$ will be attained as the observation point is located at $s_{10}\epsilon L_1$ and $s_{20}\epsilon L_2$, accordingly that influenced by $g_2{}'(s_2)$ at $s_2\epsilon L_2$. Here, two bi-elastic parameters are established, as follows:

$$\lambda_1=\frac{G_1-G_2}{G_2+\kappa_2 G_1}\ ,\lambda_2=\frac{\kappa_2 G_1-\kappa_1 G_2}{G_1+\kappa_1 G_2} \tag{29}$$

By changing the subscript 1 to 2 and 2 to 1 in δ_1 and δ_2. The SIEs for crack-L_1 in the upper part of two bonded half-planes yield

$$\begin{aligned}[N(s_{10})+iT(s_{10})]_1 &= [N(s_{10})+iT(s_{10})]_{11}+[N(s_{10})+iT(s_{10})]_{12}\\ &= \frac{1}{\pi}\int_{L_1}\frac{g_1{}'(s_1)ds_1}{s_1-s_{10}}+\frac{1}{\pi}\int_{L_1}\mu_1(s_1,s_{10})g_1{}'(s_1)ds_1\\ &+\frac{1}{\pi}\int_{L_1}\mu_2(s_1,s_{10})\overline{g_1{}'(s_1)}\,ds_1+\frac{1}{\pi}\int_{L_2}\frac{g_2{}'(s_2)ds_2}{s_2-s_{10}}+\\ &\frac{1}{\pi}\int_{L_2}M_1(s_2,s_{10})g_2{}'(s_2)ds_2+\frac{1}{\pi}\int_{L_2}M_2(s_2,s_{10})\overline{g_2{}'(s_2)}\,ds_2. \end{aligned} \tag{30}$$

The SIEs for crack-L_2 in the lower part of two bonded half-planes yield

$$\begin{aligned}[N(s_{20})+iT(s_{20})]_2 &= [N(s_{20})+iT(s_{20})]_{22}+[N(s_{20})+iT(s_{20})]_{21}\\ &= (1+\lambda_2)\frac{1}{\pi}\int_{L_2}\frac{g_2{}'(s_2)ds_2}{s_2-s_{20}}+\frac{1}{\pi}\int_{L_2}B_1(s_2,s_{20})g_2{}'(s_2)ds_2\\ &+\frac{1}{\pi}\int_{L_2}B_2(s_2,s_{20})\overline{g_2{}'(s_2)}\,ds_2+(1+\delta_2)\frac{1}{\pi}\int_{L_1}\frac{g_1{}'(s_1)ds_1}{s_1-s_{20}}\\ &+\frac{1}{\pi}\int_{L_1}B_3(s_1,s_{20})g_1{}'(s_1)ds_1+\frac{1}{\pi}\int_{L_1}B_4(s_1,s_{20})\overline{g_1{}'(s_1)}\,ds_1 \end{aligned} \tag{31}$$

where:

$$\begin{aligned}M_1(s_2,s_{10}) &= \frac{\exp(i\alpha)}{2}\left\{\lambda_1\left[\frac{1}{\bar{T}_{s_2}-T_{s_{10}}}+\frac{1}{T_{s_2}-\bar{T}_{s_{10}}}+\frac{\bar{T}_{s_{10}}-\bar{T}_{s_2}}{(T_{s_2}-\bar{T}_{s_{10}})^2}\right]\right\}\\ &+\frac{\exp(i\alpha)}{2}\left\{\exp(-2i\alpha)\left[\lambda_1\left(-\frac{1}{T_{s_2}-\bar{T}_{s_{10}}}+\frac{\bar{T}_{s_2}-3\bar{T}_{s_{10}}}{\left(T_{s_2}-\bar{T}_{s_{10}}\right)^2}+\frac{2T_{s_{10}}\left(T_{s_2}-\bar{T}_{s_2}\right)}{\left(T_{s_2}-\bar{T}_{s_{10}}\right)^3}\ \frac{2\bar{T}_{s_{10}}(\bar{T}_{s_2}-\bar{T}_{s_{10}})}{(T_{s_2}-\bar{T}_{s_{10}})^3}\right)+\right.\right.\\ &\left.\left.\lambda_2\left(\frac{1}{T_{s_2}-\bar{T}_{s_{10}}}\right)\right]\right\} \end{aligned}$$

$$M_2(s_2,s_{10}) = \frac{\exp(-i\alpha)}{2}\left\{\lambda_1\left[\frac{1}{\bar{T}_{s_2}-T_{s_{10}}}+\frac{T_{s_{10}}-T_{s_2}}{(\bar{T}_{s_2}-T_{s_{10}})^2}+\frac{1}{T_{s_2}-\bar{T}_{s_{10}}}\right]\right\}$$
$$+\frac{\exp(-i\alpha)}{2}\left\{\exp(-2i\alpha)\left[\lambda_1\left(\frac{T_{s_{10}}-\bar{T}_{s_{10}}}{(T_{s_2}-\bar{T}_{s_{10}})^2}-\frac{1}{T_{s_2}-\bar{T}_{s_{10}}}\right)\right]\right\},$$

and

$$B_1(s_2,s_{20}) = \frac{\exp(i\alpha)}{2}\left(-(1+\lambda_2)\frac{1}{T_{s_2}-T_{s_{20}}}+(1+\lambda_1)\frac{1}{\bar{T}_{s_2}-\bar{T}_{s_{20}}}\exp(-2i\alpha)\right)$$

$$B_2(s_2,s_{20}) = \frac{\exp(-i\alpha)}{2}\left\{(1+\lambda_2)\frac{1}{\bar{T}_{s_2}-\bar{T}_{s_{20}}}+\exp(-2i\alpha)\left[(1+\lambda_2)\frac{T_{s_{20}}}{(\bar{T}_{s_2}-\bar{T}_{s_{20}})^2}-(1+\lambda_1)\frac{T_{s_2}}{(\bar{T}_{s_2}-\bar{T}_{s_{20}})^2}+\right.\right.$$
$$\left.\left.(\lambda_1-\lambda_2)\left(\frac{1}{\bar{T}_{s_2}-\bar{T}_{s_{20}}}+\frac{\bar{T}_{s_{20}}}{(\bar{T}_{s_2}-\bar{T}_{s_{20}})^2}\right)\right]\right\}$$

$$B_3(s_1,s_{20}) = \frac{\exp(i\alpha)}{2}\left(-(1+\delta_2)\frac{1}{T_{s_1}-T_{s_{20}}}+(1+\delta_1)\frac{1}{\bar{T}_{s_1}-\bar{T}_{s_{20}}}\exp(-2i\alpha)\right)$$

$$B_4(s_1,s_{20}) = \frac{\exp(-i\alpha)}{2}\left\{(1+\delta_2)\frac{1}{\bar{T}_{s_1}-\bar{T}_{s_{20}}}+\exp(-2i\alpha)\left[(1+\delta_2)\frac{T_{s_{20}}}{(\bar{T}_{s_1}-\bar{T}_{s_{20}})^2}-(1+\delta_1)\frac{T_{s_1}}{(\bar{T}_{s_1}-\bar{T}_{s_{20}})^2}+\right.\right.$$
$$\left.\left.(\delta_1-\delta_2)\left(\frac{1}{\bar{T}_{s_1}-\bar{T}_{s_{20}}}+\frac{\bar{T}_{s_{20}}}{(\bar{T}_{s_1}-\bar{T}_{s_{20}})^2}\right)\right]\right\}.$$

At the particular tip of the crack, the dislocation distribution is singular, let:

$$g_j'(s_j) = \sqrt{\frac{s_j}{(a_j-s_j)}}G_j(s_j),\quad j=1,2 \tag{32}$$

Then, the SIE is numerically solved using semi-open quadrature rules accounting for both singular and regular integrals, respectively, as follows [22]:

$$\int_0^a \frac{G(s)}{s-s_k}\sqrt{\left(\frac{s}{a-s}\right)}ds = \sum_{j=1}^{M}\frac{W_jG(s_j)}{s_j-s_k} \tag{33}$$

$$\int_0^a K(s,s_k)\sqrt{\left(\frac{s}{a-s}\right)}ds = \sum_{j=1}^{M}W_jK(s_j,s_k) \tag{34}$$

where:

$$W_j = \frac{a\pi}{M}sin^2\frac{j\pi}{2M}\quad (j=1,2,\dots,M-1),$$

$$s_j = a\,sin^2\frac{j\pi}{2M}\quad (j=1,2,\dots,M),$$

$$s_k = a\,sin^2\frac{(k-0.5)\pi}{2M}\quad (k=1,2,\dots,M).$$

3. Numerical Examples and Discussions

Stress intensity factors (SIFs) at the tip of crack A_j for $j = 1, 2$ can be computed by:

$$\begin{aligned} K_{A_j} &= (K_1 - iK_2)_{A_j} \\ &= -\sqrt{2\pi} \lim_{s_j \to a_j} \sqrt{a_j - s_j}\, g_j{}'(s_j) \\ &= -\sqrt{2\pi a_j}\, G_j(a_j) \end{aligned} \quad (35)$$

Hence, it signifies.

$$\begin{aligned} K_1 &= F_{1A_j} p\sqrt{\pi a_j}, \qquad & F_{1A_j} &= -\sqrt{2} G_j(a_j), \\ K_2 &= -F_{2A_j} p\sqrt{\pi a_j}, \qquad & F_{2A_j} &= -\sqrt{2} G_j(a_j), \end{aligned} \quad (36)$$

where $F_{A_j} = (F_{1A_j} - iF_{2A_j})$, F_1 and F_2 indicate Modes I and II of the nondimensional SIFs.

3.1 Example 1

Consider multiple edge cracks emerging at the interface of two bonded half-planes towards the upper part of the planes due to normal stress, illustrated in Figure 1. R is the crack's length, e_2 signifies the distance between cracks, α_1 and α_2 denote the inclined angles, and A_1, A_2 are the crack's tip of crack 1 and 2 accordingly. When $G_2 = 0$, Eq. (26) reduces our problem to a half-plane containing an edge crack. From Table 1, it is found that the maximum percentage difference between the calculated results with Chen and Hasebe [20] is 0.085%. This validates our computation findings.

Table 1
Nondimensional SIFs at crack's tips for a single inclined edge crack in a half-plane under normal stress when inclined angle, $\alpha(°)$ varies

α (°)	5	10	15	20	25	30	35	40	45
$F_1(\alpha)^*$	0.0881	0.1494	0.2298	0.3057	0.3824	0.4631	0.5438	0.6250	0.7048
$F_1(\alpha)^{**}$	0.0881	0.1495	0.2297	0.3058	0.3825	0.4633	0.5439	0.6252	0.7054
$F_2(\alpha)^*$	0.1901	0.1849	0.2276	0.2709	0.3079	0.3358	0.3553	0.3648	0.3645
$F_2(\alpha)^{**}$	0.1901	0.1851	0.2277	0.2709	0.3080	0.3359	0.3554	0.3646	0.3648
α (°)	50	55	60	65	70	75	80	85	90
$F_1(\alpha)^*$	0.7816	0.8529	0.9204	0.9788	1.0286	1.0686	1.0978	1.1156	1.1216
$F_1(\alpha)^{**}$	0.7814	0.8532	0.9208	0.9790	1.0289	1.0686	1.0985	1.1157	1.1219
$F_2(\alpha)^*$	0.3544	0.3350	0.3057	0.2687	0.2243	0.1738	0.1186	0.0601	0.0000
$F_2(\alpha)^{**}$	0.3547	0.3352	0.3060	0.2687	0.2244	0.1734	0.1186	0.0601	0.0000

$*$ Present study
$**$ Chen and Hasebe [20]

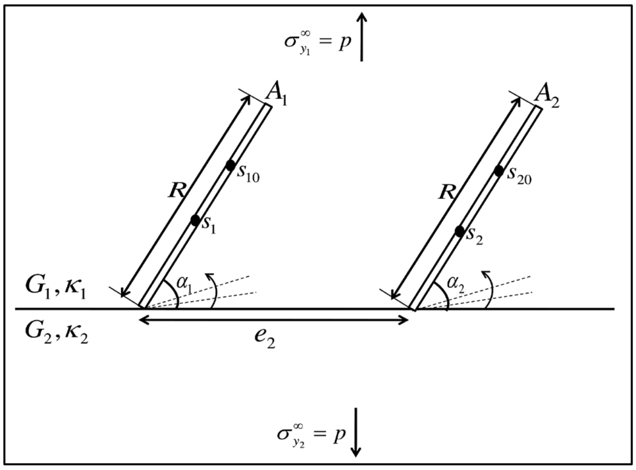

Fig. 1. Multiple inclined edge cracks in the upper half of two bonded half-planes

Figures 2 and 3 illustrate the nondimensional Modes I and II SIFs, addressing the problem in Figure 1. Figure 2(a) shows F_{1A_1} increases uniformly as α_2 increases. When $\alpha_2 > 90^{\circ}$, as $G2/G1$ increases, F_{1A_1} increases. However, F_{2A_1} decreases as $G2/G1$ increases. F_{1A_2} decreases but increases when $\alpha_2 < 80^{\circ}$ and $\alpha_2 > 80^{\circ}$ respectively as shown in Figure 2(b). It is found when $\alpha_2 > 60^{\circ}$, F_{1A_2} increases as $G2/G1$ increases. F_{2A_2} decreases when $\alpha_2 < 50^{\circ}$ but increases when $\alpha_2 > 50^{\circ}$. When $\alpha_2 > 90^{\circ}$, as $G2/G1$ increases, F_{2A_2} increases.

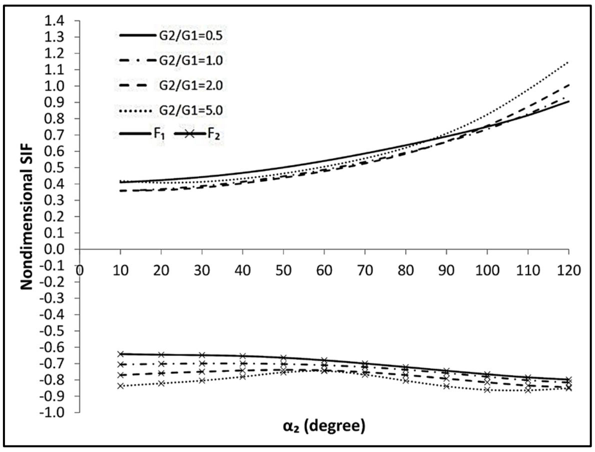

(a)

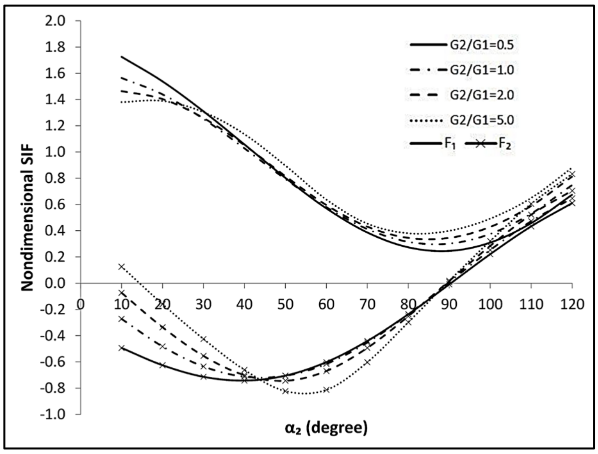

(b)

Fig. 2. Nondimensional SIFs for α_2 varies with different values of $G2/G1$ (a) SIFs at A_1 (b) SIFs at A_2

Figure 3(a) shows that as e_2/R increases, F_{1A_1} increases consistently for all values of $G2/G1$. As $G2/G1$ increases, F_{2A_1}decreases. F_{2A_1} decreases exponentially and remains constant when $e_2/R < 4$ and $e_2/R > 4$ respectively for all values of $G2/G1$. Figure 3(b) displays F_1 and F_2 at crack tip A_2 increases and decreases sharply, respectively, when $e_2/R < 3$. Furthermore, when $e_2/R > 3$, F_1 and F_2 at crack tip A_2 remain constant.

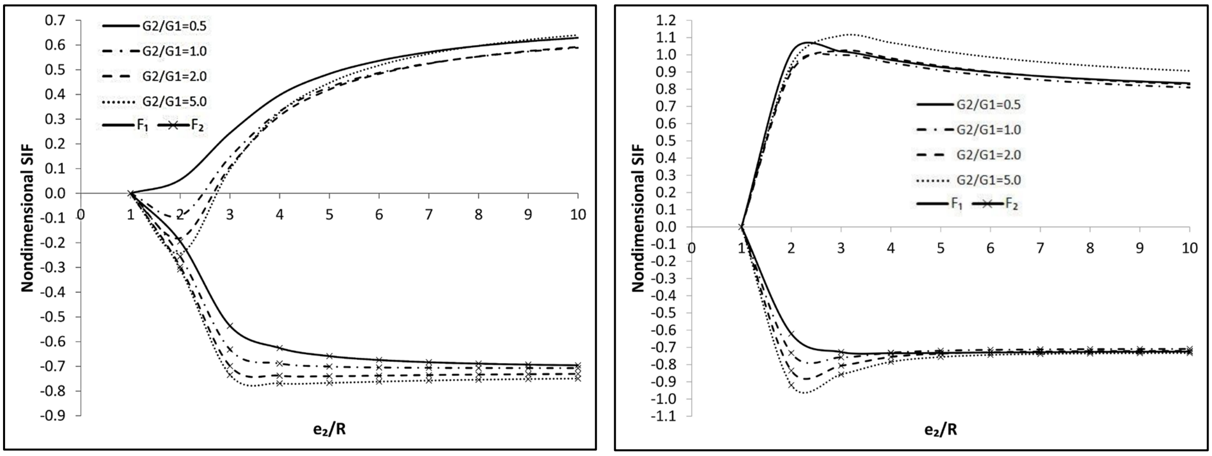

(a) (b)

Fig. 3. Nondimensional SIFs for e_2/R varies with different values of $G2/G1$(a) SIFs at A_1 (b) SIFs at A_2

3.2 Example 2

Consider multiple edge cracks originating at the interface of two bonded half-planes towards the upper and lower parts of the planes under normal stress, as shown in Figure 4. The symbols R, e_2, α_1, α_2, A_1, and A_2 are similarly described as Example 1.

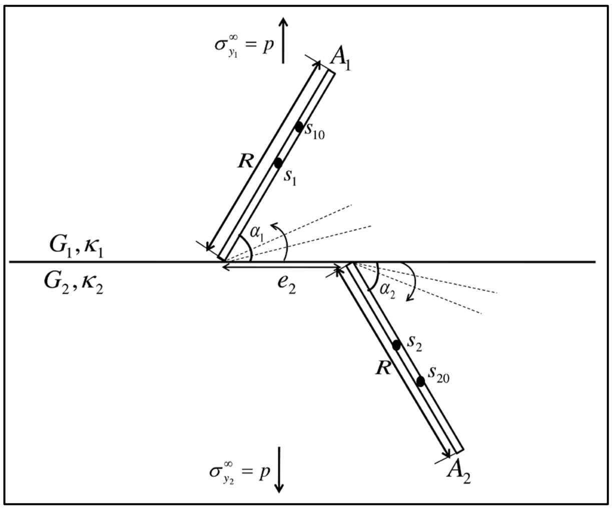

Fig. 4. Multiple inclined edge cracks in both the upper and lower parts of two bonded half-planes

Figures 5 and 6 display the nondimensional Modes I and II SIFs for the problem in Figure 4. Figure 5(a) demonstrates that as α_1 increases, F_{1A_1} decreases. When $\alpha_1 > 25^{\circ}$, as $G2/G1$ increases, F_{1A_1} increases. Meanwhile, when $\alpha_1 > 35^{\circ}$, as $G2/G1$ increases, F_{2A_1} decreases. At crack tip A_2 (see Figure 5(b)), F_1 and F_2 do not show any significant difference as α_1 increases. This is due to the uniformity of normal and shear amplitudes. F_1 and F_2 at A_2 approach zero when $G2/G1 = 2.0,\ 3.0$.

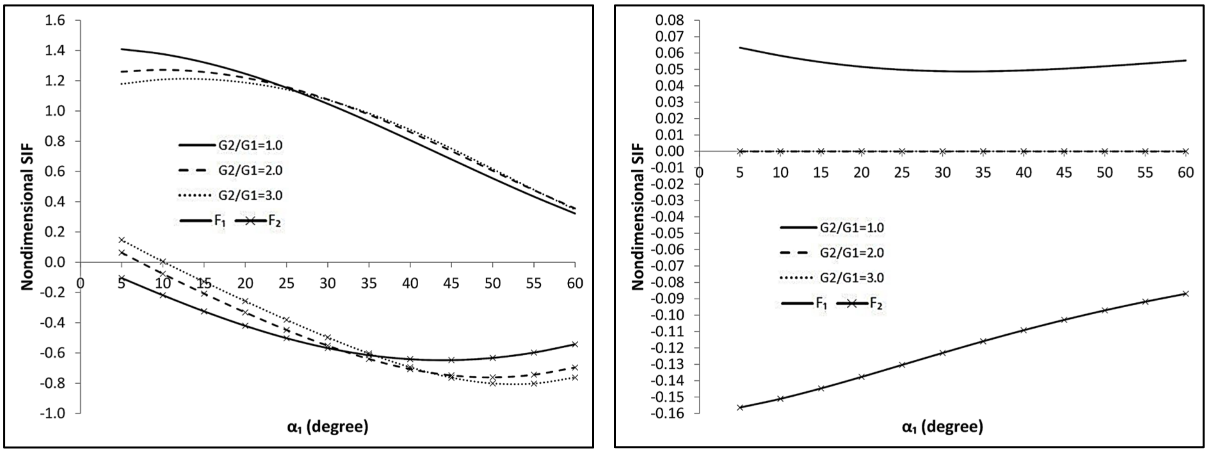

(a) (b)

Fig. 5. Nondimensional SIFs for α_2 varies with different values of $G2/G1$ (a) SIFs at A_1 (b) SIFs at A_2

Figure 6(a) demonstrates that as e_2/R increases, F_{1A_1} shows no significant difference and remains constant when $e_2/R > 4$. This is because when the distance between cracks increases, the effect of stress concentration at the crack tips decreases. As $G2/G1$ increases, F_{1A_1} increases. However, F_{2A_1} decreases as $G2/G1$ increases. Figure 6(b) illustrates F_{1A_2} and F_{2A_2} exponentially increases and decreases, respectively, when $e_2/R < 4$ for $G2/G1 = 3.0$. Moreover, for $G2/G1 = 1.0, 2.0$, F_{1A_2} and F_{2A_2} remain constant as e_2/R increases. As the distance between cracks increases, the interaction between cracks decreases and behaves like an isolated crack.

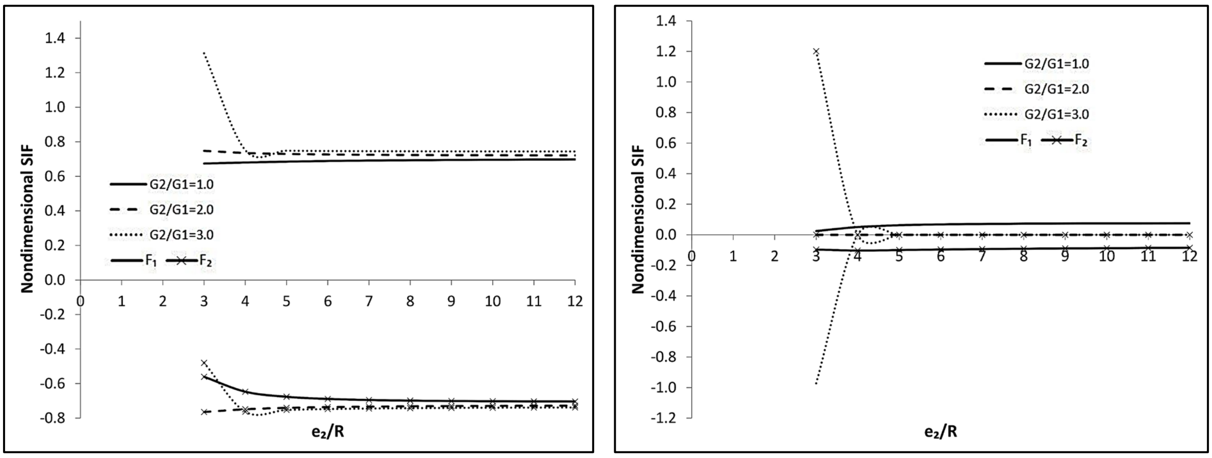

(a) (b)

Fig. 6. Nondimensional SIFs for e_2/R varies with different values of $G2/G1$ (a) SIFs at A_1 (b) SIFs at A_2

The inclination angle of the crack relative to the applied load affects the stress concentration factor, leading to an increase or decrease of SIF as the result of the combination effects of normal and shear stresses [23]. Depending on the crack's inclination angle, the ratio of elastic constants $G2/G1$ also influences the distribution of stress around the crack tip. As $G2/G1$ increases, the stress near the crack tip increases, which can lead to higher stress concentrations and thus a higher Mode I SIF. A higher shear modulus indicates that a material is stiffer against shear deformation, resulting in higher resistance to in-plane sliding. As a result, the material resists shear stress more effectively, reducing the stress concentration at the crack tip and resulting in a lower Mode II SIF [24].

The ratio of elastic constants, $G2/G1$ also affects the stress distribution at a crack tip, which corresponds to the distance between cracks. When cracks are far apart, their interactions are minimal and uniform, leading to a scenario where each crack behaves more like an isolated crack [25]. However, specific crack conditions can indeed influence the behavior of SIFs in Mode I and Mode II, which causes a behavior that differs from the common behavior. This can occur because of factors such as crack orientation, loading conditions, and the elastic constant ratios of the planes.

4. Conclusions

As a conclusion, the multiple edge cracks originating at the interface of two bonded half-planes are formulated into SIEs, and the SIEs are numerically solved using the semi-open quadrature rule. The configuration of the crack, the ratios of the elastic constants of the planes, and the inclination angle significantly influence Modes I and II SIFs. Furthermore, when dealing with multiple cracks, the distance between them can also affect the SIFs due to interaction effects, depending on the load acting on the cracks. Analyzing the behavior of the SIF near the crack tip will help engineers develop more durable and safer structures and components, thereby saving human lives and minimizing economic losses due to structural failures.

Acknowledgement

The authors thank Universiti Putra Malaysia for the financial support through Putra Grant, (GP/2023/9752700).

References

[1] Beom, H. G., and C. B. Cui. "Oblique edge crack in an anisotropic material under antiplane shear." *European Journal of Mechanics-A/Solids* 30, no. 6 (2011): 893-901. https://doi.org/10.1016/j.euromechsol.2011.05.004

[2] Hello, Gaëtan, Mabrouk Ben Tahar, and Jean-Marc Roelandt. "Analytical determination of coefficients in crack-tip stress expansions for a finite crack in an infinite plane medium." *International Journal of Solids and Structures* 49, no. 3-4 (2012): 556-566. https://doi.org/10.1016/j.ijsolstr.2011.10.024

[3] Li, Xiaotao, Xiaoyu Jiang, Xu Li, Hongda Yang, and Yanku Zhang. "Solution of an inclined crack in a finite plane and a new criterion to predict fatigue crack propagation." *International Journal of Mechanical Sciences* 119 (2016): 217-223. https://doi.org/10.1016/j.ijmecsci.2016.10.019

[4] Yu, Chuanbin, Daifeng Zou, Yu-Hao Li, Hai-Bing Yang, and Cun-Fa Gao. "An arc-shaped crack in nonlinear fully coupled thermoelectric materials." *Acta Mechanica* 229 (2018): 1989-2008. https://doi.org/10.1007/s00707-017-2099-6

[5] Hasebe, Norio. "Analysis of an orthotropic elastic plane problem of a half plane with an edge crack using a mapping function." *Acta Mechanica* 230 (2019): 2813-2826. https://doi.org/10.1007/s00707-019-02428-5

[6] Subbaiah, Arunkumar, and Ravikiran Bollineni. "Stress intensity factor of inclined internal edge crack in cylindrical pressure vessel." *Journal of Failure Analysis and Prevention* 20 (2020): 1524-1533. https://doi.org/10.1007/s11668-020-00948-0

[7] Liu, Zhuo-Er, and Yujie Wei. "An analytical solution to the stress fields of kinked cracks." *Journal of the Mechanics and Physics of Solids* 156 (2021): 104619. https://doi.org/10.1016/j.jmps.2021.104619

[8] Singh, Ritika, and Subir Das. "Mathematical study of an arbitrary-oriented crack crossing the interface of bonded functionally graded strips under thermo-mechanical loading." *Theoretical and Applied Fracture Mechanics* 117 (2022): 103170. https://doi.org/10.1016/j.tafmec.2021.103170

[9] Nordin, Muhammad Haziq Iqmal Mohd, Khairum Hamzah, Nik Mohd Asri Nik Long, Najiyah Safwa Khashi'ie, Iskandar Waini, Nurul Amira Zainal, and Sayed Kushairi Sayed Nordin. "Stress Intensity Factors for Thermoelectric Bonded Materials Weakened by an Inclined Crack." *Journal of Advanced Research in Applied Mechanics* 113, no. 1 (2024): 52-62. https://doi.org/10.37934/aram.113.1.5262

[10] Husin, Nur Hazirah, Nik Mohd Asri Nik Long, Norazak Senu, and Khairum Hamzah. "Singular integral equation for an edge crack originates at the interface of two bonded half-planes." *Acta Mechanica* (2024): 1-11. https://doi.org/10.1007/s00707-024-03993-0

[11] Jin, Xiaoqing, and Leon M. Keer. "Solution of multiple edge cracks in an elastic half plane." *International Journal of Fracture* 137 (2006): 121-137. https://doi.org/10.1007/s10704-005-3063-3

[12] Long, NMA Nik, and Z. K. Eshkuvatov. "Hypersingular integral equation for multiple curved cracks problem in plane elasticity." *International Journal of Solids and Structures* 46, no. 13 (2009): 2611-2617. https://doi.org/10.1016/j.ijsolstr.2009.02.008

[13] Hamzah, K. B., NMA Nik Long, N. Senu, and Z. K. Eshkuvatov. "Stress intensity factor for multiple cracks in bonded dissimilar materials using hypersingular integral equations." *Applied Mathematical Modelling* 73 (2019): 95-108. https://doi.org/10.1016/j.apm.2019.04.002

[14] Wang, Yong-Jian, Cun-Fa Gao, and Haopeng Song. "The anti-plane solution for the edge cracks originating from an arbitrary hole in a piezoelectric material." *Mechanics Research Communications* 65 (2015): 17-23. https://doi.org/10.1016/j.mechrescom.2015.01.005

[15] Choi, Hyung Jip. "Analysis of stress intensity factors for edge interfacial cracks in bonded dissimilar media with a functionally graded interlayer under antiplane deformation." *Theoretical and Applied Fracture Mechanics* 82 (2016): 88-95. https://doi.org/10.1016/j.tafmec.2015.12.014

[16] Stepanova, Larisa, and Pavel Roslyakov. "Multi-parameter description of the crack-tip stress field: Analytic determination of coefficients of crack-tip stress expansions in the vicinity of the crack tips of two finite cracks in an infinite plane medium." *International Journal of Solids and Structures* 100 (2016): 11-28. https://doi.org/10.1016/j.ijsolstr.2016.06.032

[17] Zhang, Jiong, Zhan Qu, Weidong Liu, and Liankun Wang. "Automated numerical simulation of the propagation of multiple cracks in a finite plane using the distributed dislocation method." *Comptes Rendus Mécanique* 347, no. 3 (2019): 191-206. https://doi.org/10.1016/j.crme.2019.01.004

[18] Moradi, I., and M. M. Monfared. "Fracture analysis of multiple curved cracks in an orthotropic FGM coating bonded to an orthotropic substrate layer." *Engineering Fracture Mechanics* 279 (2023): 109058. https://doi.org/10.1016/j.engfracmech.2023.109058

[19] Muskhelishvili, Nikolaĭ Ivanovich. *Some basic problems of the mathematical theory of elasticity*. Vol. 15. Groningen: Noordhoff, 1953.

[20] Chen, Y. Z., and Norio Hasebe. "Solution of multiple-edge crack problem of elastic half-plane by using singular integral equation approach." *Communications in Numerical Methods in Engineering* 11, no. 7 (1995): 607-617. https://doi.org/10.1002/cnm.1640110707

[21] Hamzah, K. B., NMA Nik Long, N. Senu, and Z. K. Eshkuvatov. "A new system of singular integral equations for a curvilinear crack in bonded materials." In *Journal of Physics: Conference Series* 1988, no. 1, p. 012003. IOP Publishing, 2021. https://doi.org/10.1088/1742-6596/1988/1/012003

[22] Boiko, A. V., and L. N. Karpenko. "On some numerical methods for the solution of the plane elasticity problem for bodies with cracks by means of singular integral equations." *International Journal of Fracture* 17 (1981): 381-388. https://doi.org/10.1007/BF00036190

[23] Tada, Hiroshi, Paul C. Paris, and George R. Irwin. "The stress analysis of cracks." *Handbook, Del Research Corporation* 34, no. 1973 (1973).

[24] Anderson, T. L. *Fracture Mechanics: Fundamentals and Applications, Fourth Edition (4th ed.).* Boca Raton: CRC Press, 2017. https://doi.org/10.1201/9781315370293

[25] Belov, Alexander, ed. *Applied Fracture Mechanics*. BoD–Books on Demand, 2012. https://doi.org/10.5772/2823